arXiv:1407.7472v1 [cond-mat.mes-hall] 28 Jul 2014

Electronic properties of armchair AA-stacked bilayer graphene nanoribbons

Yawar Mohammadi[1]*and Borhan Arghavani Nia[2]

[1]Young Researchers and Elite Club, Kermanshah Branch, Islamic Azad University, Kermanshah, Iran

[2]Department of Physics, Islamic Azad University, Kermanshah Branch, Kermanshah, Iran

Abstract

We study analytically, based on the tight-binding model, the electronic band structure of armchair AA-stacked bilayer graphene nanoribbons (BLGNRs) in several regimes. We apply hard-wall boundary conditions to determine the discretion dominating on the Bloch wavefunctions in the confined direction. First we consider an ideal case, perfect nanoribbons without any edge deformation, and show that their electronic properties are strongly size-dependent. We find that the narrow armchair AA-stacked BLGNRs (similar to single-layer graphene nanoribbons) may be metallic or semiconducting depending on their width determined by the number of dimer lines across the ribbon width, while the wide ribbons are metallic. Then we show that, when the edge deformation effects are taken into account, all narrow armchair AA-stacked BLGNRs become semiconducting while the wide ribbons remain metallic. We also investigate effects of an electric

*Corresponding author. Tel./fax: +98 831 427 4569, Tel: +98 831 427 4569. E-mail address: yawar.mohammadi@gmail.com

filed applied perpendicular to the nanoribbon layers and show it can be used to tune the electronic properties of these nanoribbons leading to a semiconducting-to-metallic phase transition at a critical value of the electric field which depends on the nanoribbon width. Furthermore, in all regimes, we calculate the corresponding wavefunctions which can be used to investigate and predict various properties in these nanoribbons.

Keywords: A. AA stacked BLGNR ; D. Tight-binding model; D. Wavefunction; D. Electronic band structure.

1 Introduction

Graphene, an isolated single layer of graphite, since its isolation in 2004 [1] has attracted many experimental and theoretical research activities, leading to discovery of many interesting properties [2] not been observed in the ordinary two dimensional electron gases. These unusual properties originate from the linear dependence of its spectrum and the chiral nature of its quasiparticles. The AB-stacked bilayer, and other few-layer graphene lattices, inheriting the chiral nature from graphene, also exhibit interesting properties [2, 3, 4]. Recently a new stable stacking order of few-layer graphene, few-layer graphene lattices with AA stacking order, has been observed in experimental researches [5, 6]. In these few-layer graphene lattices, each carbon atom in a top layer is located directly above the same one in the bottom layer, leading to special band structure composed of electron-, hole- and even un-doped linear graphene band structures [6]. The bilayer graphene with AA stacking order, due to this special band structure, shows many interesting properties [7, 8, 9, 10, 11, 12] not been reported for other materials.

The various experimental methods such as tailoring via a scanning tunnelling microscopy

tip [13], exfoliating from highly oriented pyrolytic graphite [14, 15, 16] and graphitizating SiC wafers [17] can be used to fabricate ribbons with finite width from single-layer graphene and from other few-layer graphene. The single-layer graphene ribbons (SLGNRs) have different width and different atomic edge terminations. Studying effects of the size and the geometry, which are found to be important in the nanotubes [18], is also necessary for the nanoribbons of single- and few-layer graphene.

The graphene nanoribbons, depending on their edge shape, are separated into two groups, armchair and zigzag graphene nanoribbons. Based on the tight-binding model investigations, all zigzag SLGNRs are metallic [19, 20]. While all armchair SLGNRs, due to the edge deformation effects and the quantum confinement coming from the finite width of the nanoribbon, are semiconducting [21, 22]. A density functional theory calculation [23], which was confirmed later by an experimental research [24], showed that not only all armchair SLGNRs but also all zigzag SLGNRs are semiconducting. Recently AA-stacked BLG nanoribbons also have been investigated [25, 26, 27, 28, 29]. In this paper we derive, by taking the edge deformations into account, a general analytical expression for the electronic band structure and the wavefunction of the armchair AA-stacked BLGNRs which can be used to investigate and predict various properties in these nanoribbons. We also show that it is possible to tune the electronic properties of the armchair AA-stacked BLGNRs via an electric field applied perpendicular to the ribbons layers.

The paper is organized as follow. In the section II, we obtain sublattice Bloch wavefunctions by imposing the hard-wall condition. Then, by making use of the tight-binding model, we present a general expression for the Schrödinger equation of the armchair AA-stacked BLGNRs which can be solved to obtain its dispersion relation. First we consider an ideal case, an

armchair AA-stacked BLGNR without any edge deformation. Then we investigate effects of the edge deformation on the dispersion relation and the wavefunction of the armchair AA-stacked BLGNRs. In the section III, we examine effects of an electric filed, applied perpendicular to the nanoribbons layers, on the electronic properties of the AA-stacked BLGNR. Finally, in the section IV, we end the paper by summary and conclusions.

2 Model Hamiltonian, electron wavefunction and band structure

In an AA-stacked BLGNR, which is composed of two SLG nanoribbons, each sublattice in the top layer is located directly above the same one in the bottom layer. Figure 1 shows a segment of an AA-stacked BLGNR with armchair atomic edge termination whose unit cell is enclosed inside the dashed lines. The unit cell contains N A-type atoms and N B-type atoms in each layer that N is the number of dimer lines across the ribbon width.

To investigate the electronic properties of a lattice structure using tight-binding model, first we must construct its Bloch wavefunction which for an AA-stacked BLGNR can be written as

$$|\Psi\rangle = c_{A_1}|\psi_{A_1}\rangle + c_{B_1}|\psi_{B_1}\rangle + c_{A_2}|\psi_{A_2}\rangle + c_{B_2}|\psi_{B_2}\rangle, \tag{1}$$

where $|\psi_{A_1}\rangle$, $|\psi_{B_1}\rangle$, $|\psi_{A_2}\rangle$ and $|\psi_{B_2}\rangle$ are the Bloch wavefunction corresponding to p^z orbital of A_1, B_1, A_2 and B_2 sublattices respectively and c_{A_1}, c_{B_1}, c_{A_2} and c_{B_2} are momentum-dependent coefficients.

The armchair AA-stacked BLGN is supposed to has infinite length (fig. 1) along the x direction. This leads to translational invariance along the x direction, allowing us to choose

plan wave basis along the x direction, $e^{ik_x x}$, for constructing sublattice Bloch wavefunctions. While the quantum confinement, coming from the finite width of the nanoribbon, breaks the spectrum of an AA-stacked BLG into a set of subbands and dominates a discretion on the amount of the momentum in the y direction. The discrete values of the momentum in the y direction, k_n, can be obtained by imposing hard-wall boundary condition which indicates that all sublattice Bloch wavefunctions at auxiliary sublattices at the both edges of the armchair AA-stacked BLGN, $y = 0$ and $y = (N+1)a/2$, must be zero. This give rises to

$$k_n = n\frac{\pi}{N+1}\frac{2}{\sqrt{3}a}, \qquad n = 1, 2, ...N. \tag{2}$$

Therefore, the normalized sublattice Bloch wavefunctions can be written as

$$\begin{aligned}
|\psi_{A_1}\rangle &= \frac{\sqrt{2}}{\sqrt{N_x(N+1)}} \sum_{x_{A_1 i}} \sum_{i=1}^{N} e^{ik_x x_{A_{1i}}} \sin(\frac{\sqrt{3}ak_n}{2} i)|p^z_{A_{1i}}\rangle, \\
|\psi_{B_1}\rangle &= \frac{\sqrt{2}}{\sqrt{N_x(N+1)}} \sum_{x_{B_1 i}} \sum_{i=1}^{N} e^{ik_x x_{B_{1i}}} \sin(\frac{\sqrt{3}ak_n}{2} i)|p^z_{B_{1i}}\rangle, \\
|\psi_{A_2}\rangle &= \frac{\sqrt{2}}{\sqrt{N_x(N+1)}} \sum_{x_{A_2 i}} \sum_{i=1}^{N} e^{ik_x x_{A_{2i}}} \sin(\frac{\sqrt{3}ak_n}{2} i)|p^z_{A_{2i}}\rangle, \\
|\psi_{B_2}\rangle &= \frac{\sqrt{2}}{\sqrt{N_x(N+1)}} \sum_{x_{B_2 i}} \sum_{i=1}^{N} e^{ik_x x_{B_{2i}}} \sin(\frac{\sqrt{3}ak_n}{2} i)|p^z_{B_{2i}}\rangle,
\end{aligned} \tag{3}$$

where N_x is the number of unit cells along the x direction and $x_{A_{1i}}$ is the x-coordinate of A_1 in the i-th dimer line across the ribbon width. The spectrum and the wavefunction are derived by solving the Schrödinger equation [30] which, for an armchair AA-stacked BLGNR, reduces to a 4×4 matrix equation as

$$\begin{pmatrix}
H_{A_1A_1} - E & H_{A_1B_1} & H_{A_1A_2} & H_{A_1B_2} \\
H_{B_1A_1} & H_{B_1B_1} - E & H_{B_1A_2} & H_{B_1B_2} \\
H_{A_2A_1} & H_{A_2B_1} & H_{A_2A_2} - E & H_{A_2B_2} \\
H_{B_2A_1} & H_{B_2B_1} & H_{B_2A_2} & H_{B_2B_2} - E
\end{pmatrix}
\begin{pmatrix}
c_{A_1} \\ c_{B_1} \\ c_{A_2} \\ c_{B_2}
\end{pmatrix} = 0, \tag{4}$$

where $H_{A_pA_q} = \langle\psi_{A_p}|\mathcal{H}|\psi_{A_q}\rangle$, $H_{B_pB_q} = \langle\psi_{B_p}|\mathcal{H}|\psi_{B_q}\rangle$ and $H_{A_pB_q} = H^*_{B_qA_p} = \langle\psi_{A_p}|\mathcal{H}|\psi_{B_q}\rangle$ where p and q are 1 and 2. Here, $\mathcal{H}$ is the Hamiltonian of an armchair AA-stacked BLGNR lattice.

2.1 Perfect nanaoribbons

First we consider an ideal case, a perfect armchair AA-stacked BLGNR *without any edge deformation*. If we apply the nearest-neighbor tight-binding approximation to obtain the elements of the matrix equation (Eq. 4)), we get

$$\begin{aligned} H^0_{A_1B_1} = H^{0*}_{B_1A_1} = H^0_{A_2B_2} = H^{0*}_{B_2A_2} = f^0_n(k_x), \\ H^0_{A_1A_1} = H^0_{B_1B_1} = H^0_{A_2A_2} = H^0_{B_2B_2} = \varepsilon_{p^z}, \\ H^0_{A_1A_2} = H^0_{A_2A_1} = H^0_{B_1B_2} = H^0_{B_2B_1} = \gamma, \\ H^0_{A_1B_2} = H^0_{B_1A_2} = H^0_{A_2B_1} = H^0_{B_2A_1} = 0, \end{aligned} \tag{5}$$

where $f^0_n(k_x) = -t(e^{-ik_xa} + 2\cos(n\frac{\pi}{N+1})e^{ik_xa/2})$, $t \sim 3eV$ [11] and $\gamma \sim 0.2eV$ [31, 32] are the nearest-neighbor intralyer and interlayer hopping energies and ε_{p^z} is energy of the p^z orbital which can be kept to zero as the energy reference. In the above equations and hereafter, the superscript 0 indicates that these quantities refer to a perfect armchair AA-stacked BLGNR, an armchair AA-stacked BLGNR ribbon without any edge deformation. Here, we have used $S_{A_pA_p} = \langle\psi_{A_p}|\psi_{A_p}\rangle = 1$, $S_{B_pB_p} = \langle\psi_{B_p}|\psi_{B_p}\rangle = 1$ and $S_{A_pB_q} = S^*_{B_qA_p} = \langle\psi_{A_p}|\psi_{B_q}\rangle \approx 0$ [33] where p and q are 1 and 2. It is the so-called orthogonal tight-binding schemes. Thus, the spectrum and the wavefunction become

$$\begin{aligned} E^{0s\lambda}_n &= s\gamma + \lambda|f^0_n(k_x)|, \\ |\Psi\rangle^{0s\lambda}_n &= \frac{1}{2}([|\psi_{A_1}\rangle + \lambda\frac{f^{0*}_n(k_x)}{|f^0_n(k_x)|}|\psi_{B_1}\rangle] + s[|\psi_{A_2}\rangle + \lambda\frac{f^{0*}_n(k_x)}{|f^0_n(k_x)|}|\psi_{B_2}\rangle]), \end{aligned} \tag{6}$$

where $s = \pm$ are band indexes and $\lambda = \pm$ denote the conduction and the valance bands. It is evident from Eq. (6) that the spectrum of an armchair AA-stacked BLGNR is composed of the spectrums of two armchair SLGNRs denoted by $s = +$ and $s = -$ which have been shifted along energy axis by $+\gamma$ and $-\gamma$ respectively. This make the electronic band structure of armchair AA-stacked BLGNRs different from that of SLGNRs. Moreover, as Eq. (6) shows, since all A_1, B_1, A_2, and B_2-atoms of each dimer contribute equivalently in constructing wavefunction, the electron density of sates on all atoms of each dimer are equal and the electron density of states only depend on the distance from the armchair edge. This can be examined by a STM image.

The armchair AA-stacked BLGNRs, depending on their width, may be metallic or semiconducting. Figure 2 shows our results for the energy gap of different armchair AA-stacked BLGNRs as a function of their width. According to the width dependence of the energy gap, the armchair AA-stacked BLGNRs are separated into three groups denoted by $N = 3m$, $N = 3m + 1$ and $N = 3m + 2$ where N is the number of dimer lines across the ribbon width (figure 1) and m is a positive integer number. This figure shows that all armchair AA-stacked BLGNRs with $N = 3m + 2$ are metallic. This is understood by the fact that for these nanoribbons, $f^0_{n=2m+2}(k_x = 0) = -2t(\cos(\frac{(2m+2)\pi}{3m+3}) + \frac{1}{2}) = 2t(\cos(\frac{2\pi}{3}) + \frac{1}{2}) = 0$. This means that, for this group of armchair AA-stacked BLGNRs, the upmost valance and the lowest conduction sub-bands of bands with same s-index band always touch each other at $k_x = 0$, leading to metallic behavior.

Moreover, this figure shows that the armchair AA-stacked BLGNRs with $N = 3m$ and $N = 3m + 1$ may be metallic or semiconducting depending on their width. This is different from what has been reported for armchair SLGNRs [19, 20, 21, 22]. This can be explained as follows; It is evident that for $N = 3m$ and $N = 3m + 1$ all $f^0_n(k_x = 0) \neq 0$, inducing an

energy gap between the sub-bands with same s-index band. Moreover, as mentioned above, the spectrum of an AA-stacked BLGNR is composed of two SLGNR spectrums denoted by $s = +$ and $s = -$ which have been shifted along energy axis by $+\gamma$ and $-\gamma$ respectively. Therefore, an armchair AA-stacked BLGNR is semiconducting if the induced bad gaps, the minimum of $2t|1 + 2\cos(\frac{n\pi}{N+1})|$ with $n = 1, 2, ...N$ which is $2t|1 + 2\cos(\frac{(2m+1)\pi}{N+1})|$, is larger than 2γ and it is metallic when it isn't. This can be seen in fig. 3 and fig. 4. This is dependent on the width of the nanoribbon. When the nanoribbon is narrow, the induced energy gap is large enough to be larger than 2γ, so the nanoribbon become semiconducting. While when the width of the nanoribbon increases, the induced energy gap becomes smaller than 2γ leading to the metallic behavior. Notice that for both groups of semiconducting armchair AA-stacked BLGNRs ($N = 3m$ and $N = 3m + 1$), there is a critical width that if the nanoribbon width exceeds that the nanoribbon becomes metallic.

2.2 Edge deformation effects

The nanoribbons have unpaired covalent carbon bonds at their edges making these material unstable [21]. These dangling bonds can be passivated by hydrogen atoms or other kinds of atoms or molecules [19, 22, 23], leading to a stable state [21]. The first-principle calculations showed that the carbon bond-lengths at the edges of the hydrogenated SLGNRs [23] and the large aromatic molecules [34] are shorter than those in the middle regions. Furthermore, an analytical calculation[35], based on the tight-binding model, found that a decreasing about 3 - 4 percent in the carbon bond-lengths could induce an increasing about 12 percent in the hopping integral between p^z orbitals. These edge deformation effects must be taken into account to achieve a real understanding about electronic properties of the nanoribbons. Here, similar to

the previous works [22, 23] which studied the armchair SLGNRs, we suppose that all intralayer hopping energy deviations are negligible except those occur between the sublattices at $i = 1$ dimer line or between those at $i = N$ dimer line. Therefore, we have

$$\begin{aligned} \delta H_{A_pB_p} &= \delta H^*_{B_pA_p} = \delta f_n(k_x) \\ &= -\frac{2\delta t e^{-ik_x a}}{N+1}(\sin^2(\frac{n\pi}{N+1}) + \sin^2(N\frac{n\pi}{N+1})) \\ &= -\frac{4\delta t e^{-ik_x a}}{N+1}\sin^2(\frac{n\pi}{N+1}), \end{aligned} \tag{7}$$

where δt is the nearest-neighbor intralayer hopping energy deviation and $p = 1$ and 2. So, the spectrum and the wavefunction of the edge-deformed armchair AA-stacked BLGNR are given by

$$\begin{aligned} &E_n^{s\lambda} = s\gamma + \lambda|f_n(k_x)|, \\ &|\Psi\rangle_n^{s\lambda} = \frac{1}{2}([|\psi_{A_1}\rangle + \lambda\frac{f_n^*(k_x)}{|f_n(k_x)|}|\psi_{B_1}\rangle] + s[|\psi_{A_2}\rangle + \lambda\frac{f_n^*(k_x)}{|f_n(k_x)|}|\psi_{B_2}\rangle]), \end{aligned} \tag{8}$$

where $f_n(k_x) = f_n^0(k_x) + \delta f_n(k_x)$ and so

$$E_n^{s\lambda} = s\gamma + \lambda\sqrt{|f_n^0(k_x)|^2 + |\delta f_n(k_x)|^2 + 2Re(f_n^0(k_x)\delta f_n^*(k_x))}. \tag{9}$$

It is easy to show that the band gap of the deformed nanoribbon is a direct one which occurs at $k_x = 0$. The band gap occurs between the first conduction and valance bands with $n = 2m+1$ when $N = 3m$ or $N = 3m+1$ and between the subbands with $n = 2m+2$ when $N = 3m+2$. The analytical results for the energy gap, obtained from Eq. (9) in terms of the δt up to the first order ($|\delta f_n(k_x)|^2 \to 0$), are given by

$$\Delta_N^{BLG} = [\Delta_N^{SLG} - 2\gamma]\theta(\Delta_N^{SLG} - 2\gamma), \tag{10}$$

where Δ_N^{SLG} are the energy gap of the armchair SLGNR with same width which are

$$\Delta_{N=3m}^{SLG} = 2t|1 + 2\cos(\frac{2m+1}{N+1}\pi)| - \frac{8\delta t}{N+1}\sin^2(\frac{m}{N+1}\pi),$$

$$\Delta^{SLG}_{N=3m+1} = 2t|1 + 2\cos(\frac{2m+1}{N+1}\pi)| + \frac{8\delta t}{N+1}\sin^2(\frac{m+1}{N+1}\pi),$$
$$\Delta^{SLG}_{N=3m+2} = \frac{6\delta t}{N+1}. \quad (11)$$

Our results at zero limit of the interlayer hopping energy reduce to the results which have been reported for the armchair SLGNRs [22, 23]. Figure 5 shows our results for the energy gap of the edge-deformed armchair AA-stacked BLGNRs as a function of their width obtained from Eq. (9). We see that, due to the edge deformation effects which couple electron and hole states with equal momentum, a band gap opens in the band structure of the narrow armchair AA-stacked BLGNRs with $N = 3m + 2$. Furthermore, the energy gap of the the armchair AA-stacked BLGNRs with $N = 3m + 1$ increases, while that of the armchair AA-stacked BLGNRs with $N = 3m$ decreases. Hence, all narrow edge-deformed armchair AA-stacked BLGNRs become semiconducting while the wide ribbons remain metallic. Moreover, Eq. (8) shows that, when the edge deformation effects are take into account, the magnitude of the wavefunction on all sublattices of the edge-deformed armchair AA-stacked BLGNRs remain unchanged indicating that the local density of state on all sublattices of edge-deformed armchair AA-stacked BLGNRs are equal to those of the perfect nanoribbons.

3 Effects of a perpendicular electric field

Here we investigate effects of a perpendicular electric field on the electronic properties of armchair AA-stacked BLGNRs. Applying a perpendicular electric field creates a potential $+V$ in the top layer and a potential $-V$ in the bottom one. So the corresponding Schrödinger equation can be obtained from Eq. (4) by just substituting

$$H_{A_1A_1} \to H_{A_1A_1} + V \quad , \quad H_{B_1B_1} \to H_{B_1B_1} + V,$$
$$H_{A_2A_2} \to H_{A_2A_2} - V \quad , \quad H_{B_2B_2} \to H_{B_2B_2} - V. \tag{12}$$

If we take effects of the edge deformation into account, this yields

$$E_n^{Vs\lambda} = s\gamma^{'} + \lambda|f_n(k_x)|,$$
$$|\Psi\rangle_n^{Vs\lambda} = \frac{\gamma}{2\sqrt{\gamma'(\gamma'-V)}}([|\psi_{A_1}\rangle + \lambda\frac{f_n^*(k_x)}{|f_n(k_x)|}|\psi_{B_1}\rangle] + s\frac{\gamma^{'}-V}{\gamma}[|\psi_{A_2}\rangle + \lambda\frac{f_n^*(k_x)}{|f_n(k_x)|}|\psi_{B_2}\rangle]) \tag{13}$$

where $\gamma^{'} = \sqrt{\gamma^2 + V^2}$. These results at the zero limit of the electric potential, $V \to 0$, reduce to our result which has been introduced in Eq. (8). Notice that effects of the perpendicular electric field on the electronic band structure can be taken into account only by a renormalization of the interlayer hoping energy to a new value which depends on the electrical potential as $\gamma^{'} = \sqrt{\gamma^2 + V^2}$. This shows that one can tune the electronic structure of the armchair AA-stacked BLGNRs by an electric filed applied perpendicular to layers. Figure 6 shows our results for the energy gap of the armchair AA-stacked BLGNRs with $N = 3m + 1$ for different values of the vertical electric field, $V = 0.0$, $V = 1.0\gamma$ and $V = 2.0\gamma$. Notice that if the amount of the electric field increase the energy gap of the nanoribbon decreases leading to a semiconducting-to-metallic phase transition at a special value of the electric field. This indicates that these nanoribbons can be used as current switchers. Moreover, this phase transition can lead to other interesting properties, which have been reported for undoped AA-stacked BLG coming from the nonzero density of state at Fermi energy, such as coherent plasmon dispersion which can exist even in the presence of doping[36]. Based on our results, in an armchair AA-stacked BLGNR this plasmon dispersion can be controlled electrically.

As another result of Eq. (8), we mention that, in the presence of a perpendicular electric field, the electron-density of states at top and bottom layer becomes different. The reason is that the perpendicular electric field breaks the symmetry of two layers leading to different probability amplitudes on top and bottom layer sublattices.

4 Summary and conclusions

In summary, we derive analytical relations for the electronic band structure and the wavefunction of AA-stacked BLGNRs with armchair edge shapes using tight-binding model in several regimes. First we considered an ideal case, armchair AA-stacked BLGNRs without any edge deformation. We found that the electronic properties of these nanoribbons, similar to armchair SLGNRs, depend on their width but with several differences; All ribbons with $N = 3m + 2$ are metallic, while for ribbons with $N = 3m$ and $N = 3m + 1$, by increasing the ribbon width a semiconducting-to-metallic phase transition takes place, where N is the number of dimer lines across the ribbon width. In addition, we investigate edge deformation effects and showed that all narrow edge-deformed armchair AA-stacked BLGNRs become semiconducting while the wide ribbons remain metallic. Moreover, we showed that our analytical results for the electron wavefunction and the band structure at the limit of zero interlayer hopping energy reduces to the results reported for the armchair SLGNRs. Finally, we considered the effect of a perpendicular electric field on the electronic properties of the armchair AA-stacked BLGNRs. We showed that one can tune the electronic band structure of the armchair AA-stacked BLGNRs leading to some interesting properties which have been reported for an AA-stacked BLG lattice.

References

[1] K. S. Novoselov, A. K. Geim, S. M. Morozov, D. Jiang, Y. Zhang, S. V. Dubonos, I. V.Grigorieva, and A. A. Firosov, Science 306 (2004) 666-669.

[2] A. H. Castro Neto, F. Guinea, N. M. R. Peres, K. S. Novoselov, and A. K. Geim Rev. Mod. Phys. 81 (2009) 109-162.

[3] N. M. R. Peres, Rev. Mod. Phys. 82 (2010) 2673-2700.

[4] S. Das Sarma, S. Adam, E. H. Hwang, E. Rossi, Rev. Mod. Phys. 83 (2011) 407-470.

[5] Z. Liu, K. Suenaga, P. J. Harris, S. Iijima, Phys. Rev. Lett. 102 (2009) 015501-015504.

[6] J. Borysiuk, J. Soltys, J. Piechota, Journal of Applied Physics 109 (2011) 093523-093527.

[7] T. Ando, J. Phys.: Conf. Ser. 302 (2011) 012015-012027.

[8] Y. -F. Hsu, G. -Y. Guo, Phys. Rev. B 82 (2011) 165404-165411.

[9] E. Prada, P. San-Jose, L. Brey, H. Fertig, Solid State Commun. 151 (2011) 1065-1070.

[10] A. L. Rakhmanov, A. V. Rozhkov, A. O. Sboychakov, and F. Nori Phys. Rev Lett. 109 (2012) 206801-206805.

[11] C. J. Tabert, E. J. Nicol, Phys. Rev. B 84 (2012) 075439-075450.

[12] L. Brey, H. A. Fertig, Phys. Rev. B 87 (2013) 115411-115418.

[13] H. Hiura, Appl. Surf. Sci. 222 (2004) 374-381.

[14] K. S. Novoselov, A. K. Geim, S. M. Morozov, D. Jiang, M. I. Katsnelson, I. V. Grigorieva, S. V. Dubonos, and A. A. Firosov, Nature 438 (2005) 197-200.

[15] Y. B. Zhang, Y. W. Tan, H. L. Stormer, and P. Kim, Nature 438 (2005) 201-204.

[16] J. S. Bunch, A. M. Van der Zande, S. S. Verbridge, I. W. Frank, D. M. Tanenbaum, J. M. Parpia, H. G. Craighead, and P. L. McEuen, Science 315 (2007) 490-493.

[17] C. Berger, Z. M. Song, X. B. Li, X. S. Wu, N. Brown, C. Naud, D. Mayou, T. B. Li, J. Hass, A. N. Marchenkov, E. H. Conral, P. N. First, and W. A. de Heer, Science 312 (2006) 1191-1196.

[18] R. Saito, G. Dresselhaus, and M. S. Dresselhaus, Physical Properties of Carbon Nanotubes, Imperial College, London, 1998.

[19] M. Ezawa, Phys. Rev. B 73 (2006) 045432-045439.

[20] L. Brey and H. A. Fertig, Phys. Rev. B 73 (2006) 235411-235415.

[21] A. Rozhkov, V. S. Savel'ev, and F. Nori, Phys. Rev. B 79 (2009) 125420-125429.

[22] H. Zheng, Z. Wang, T. Luo, Q. Shi, and J. Chen, Phys. Rev. B 75 (2007) 165414-165419.

[23] Y-. W. Son, M. L. Cohen, and S. G. Louie, Phys. Rev Lett. 97 (2006) 216803-216806.

[24] M. Y. Han, B. Ozyilmaz, Y. Zhang, and P. Kim Phys. Rev Lett. 98 (2007) 206805-206808.

[25] K. M. M. Habib, F. Zahid, and R. K. Lake, Appl. Phys. Lett. 98 (2011) 192112-192114.

[26] N. Xu, B. L. Wang, D. Shi, and C. Zhang. Solid State Cmmun. 152 (2012) 994-998.

[27] X. Zhong, R. Pandey, and S. P. Karna, Carbon 50 (2012) 784-790.

[28] M. Z. Ahmed, 2013, arXiv:1306.4693.

[29] E. S. Morell, R. Vergara, M. Pacheco, L. Brey, and L. Chico, Phys. Rev. B 89 (2014) 205405-205411.

[30] G. Grosso and G. P. Parravicini, olid State Physics, Academic Press, 200, p.146.

[31] Y. Xu, X. Li, and J. Dong, Nanotechnology 21 (2010) 065711-065717.

[32] I. Lobato and B. Partoens, Phys. Rev. B 83 (2011) 165429-165437.

[33] S. Reich, J. Maultzsch, C. Thomsen, and P. Ordejón, Phys. Rev. B 66 (2002) 035412-035416.

[34] C. A. Coulson, J. Phys. Chem. 56 (1952) 311-316.

[35] D. Porezag, Th. Frauenheim Th., Th. Köhler, G. Seifert, and R. Kaschner, Phys. Rev. B 51 (1995) 12947–12957.

[36] R. Roldan, L. Brey, Phys. Rev. B 88 (2013) 115420-115426.

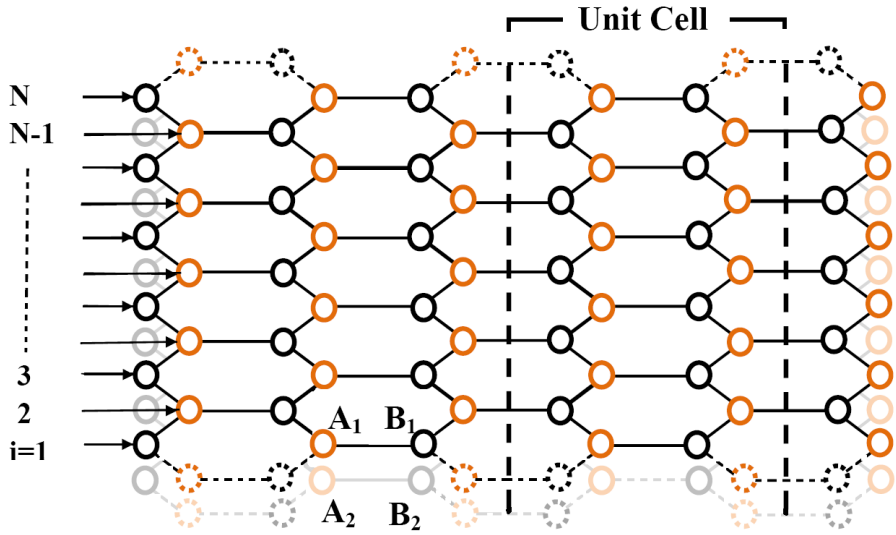

Figure 1: Structure of an armchair AA-stacked BLGNR whose unit cell is limited by two dashed lines, consisting $4N$ sublattices which N is the number of the dimer lines across its width. The dashed circles at both edges of the ribbon denote auxiliary sublattices where the sublattice wavefunctions are supposed to be zero there. The sublattices in the top layer are indicated by subscript 1, A_1 and B_1, and those in the bottom layer by subindex 2, A_2 and B_2.

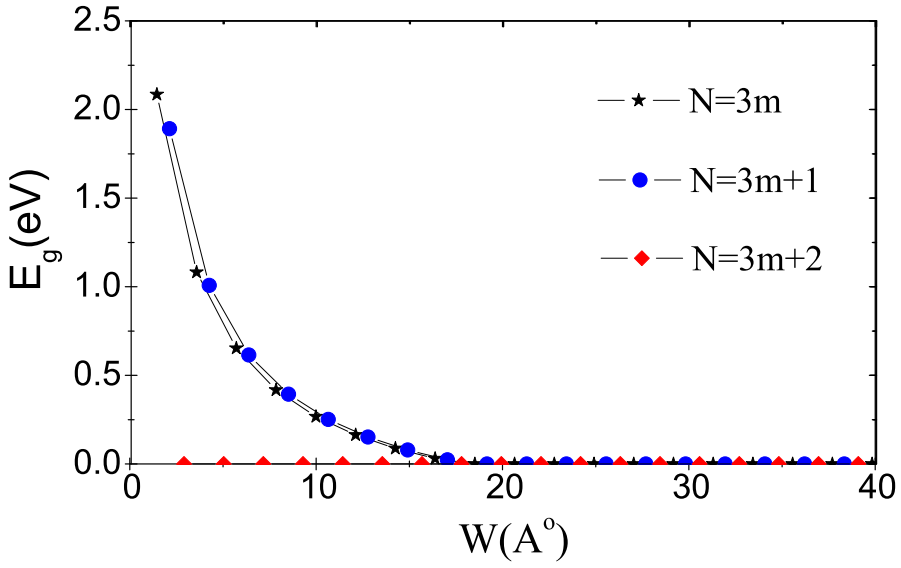

Figure 2: The energy gap of the perfect armchair AA-stacked BLGNRs as a function of their width. Here the edge deformation effects have been neglected. Three different groups have been indicated by the number of the dimer lines across their width, $N = 3m$, $N = 3m + 1$ and $N = 3m + 2$.

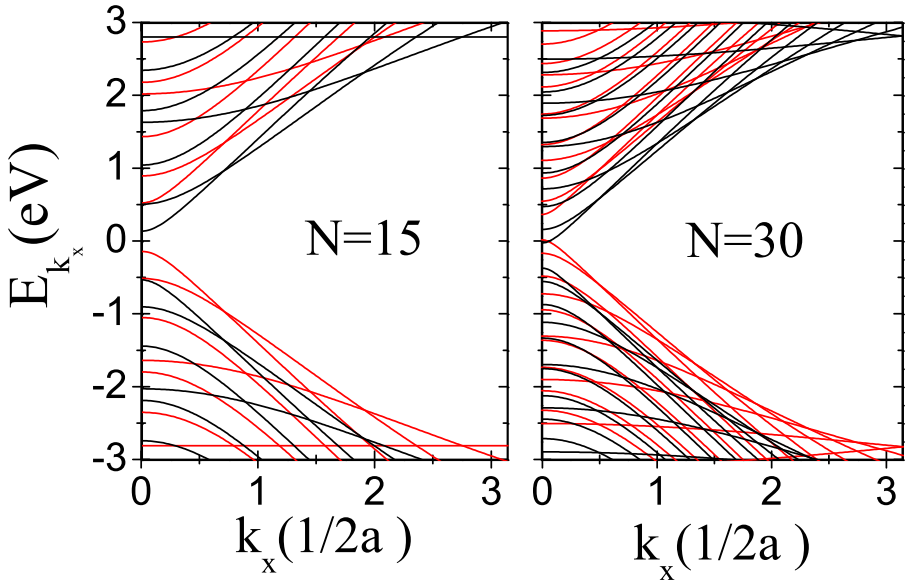

Figure 3: The electronic band structure of two armchair AA-stacked BLGNRs with $N = 3m$, $N = 15$ (left panel) and $N = 30$ (right panel). The red and black curves show the subbands with $s = +$ and $s = -$ respectively. Notice that for the armchair AA-stacked BLGNRs with $N = 30$, the induced band gap is filled by the shifted subbands, leading to the metallic behavior.

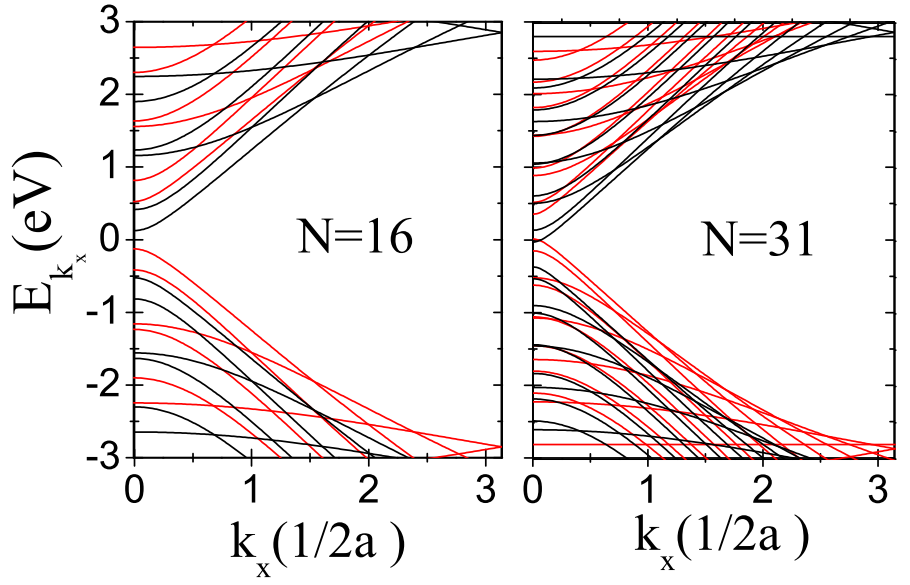

Figure 4: Same as figure 3 but with $N = 3m + 1$.

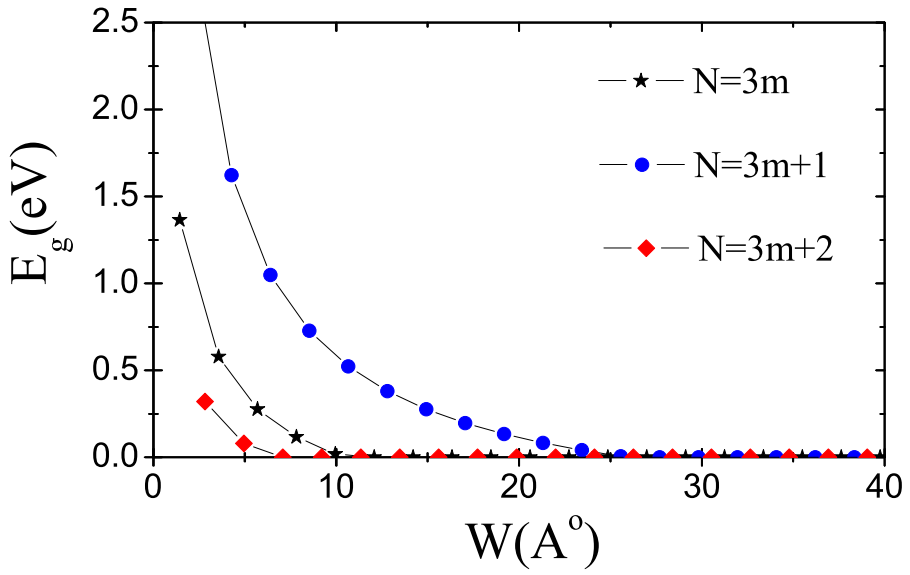

Figure 5: The energy gap of the edge-deformed armchair AA-stacked BLGNRs as a function of their width. Three different groups have been indicated by the number of the dimer lines across their width, $N = 3m$, $N = 3m + 1$ and $N = 3m + 2$.

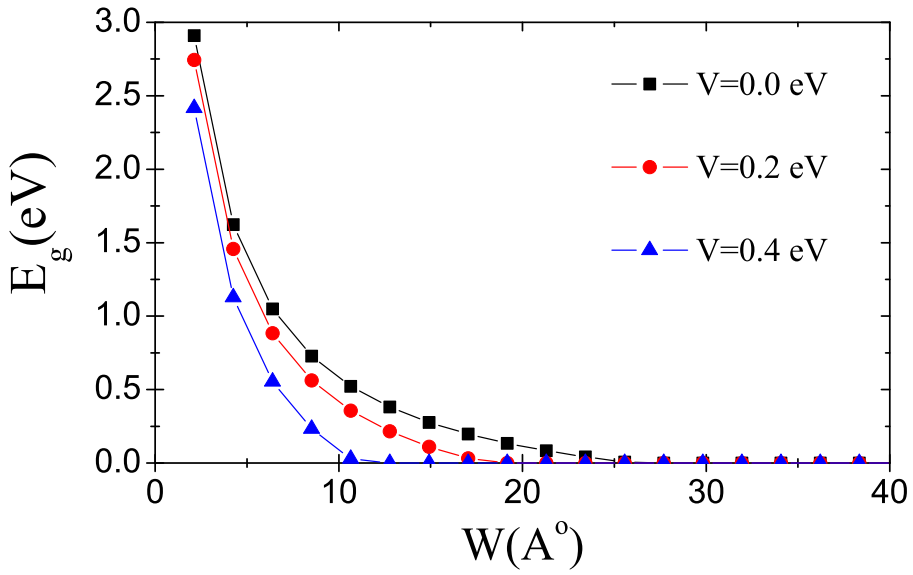

Figure 6: The energy gap of the edge-deformed armchair AA-stacked BLGNRs with $N = 3m+1$ as a function of their width in the presence of a vertical electric field, for three different values of the electrical potential: $V = 0.0eV$, $V = 0.2eV$ and $V = 0.4eV$.